THEORETICAL AND EXPERIMENTAL STUDIES OF THE FEL-BEAM INTERACTION IN A STORAGE RING

G. De Ninno, D. Nutarelli, D. Garzella, M. E. Couprie
SPAM, 91 191 Gif sur Yvette, France, LURE, 91 898 Orsay Cédex, France
M. Billardon, ESPCI, 75 231 Paris Cédex, France

Abstract

The Free Electron Laser (FEL) is a coherent and tuneable radiation source generated by the energy exchange between a relativistic electron beam and an electromagnetic wave stored in an optical cavity. The light pulses interact many times with the same electron bunch and the shape of the electron bunch is modified. An original theoretical approach is here proposed taking into account that only the electrons which superimpose with the laser pulse are perturbed. Such a model can be applied to the study of a large class of physical phenomena and, in particular, to storage ring based FELs. The model is applied to the case of the ELETTRA FEL and its reliability is confirmed by a set of experimental observations performed on the ACO and Super-ACO FELs at LURE in Orsay.

1 INTRODUCTION

A storage ring Free Electron Laser (FEL) [1] is based on the interaction of a relativistic electron beam with the sinusoidal permanent magnetic field of an undulator. The laser oscillations starts from the undulator radiation at the wavelength λ_{laser} given by

$$\lambda_{laser} = \frac{\lambda_0}{2\gamma^2}\left(1 + \frac{K^2}{2}\right) \qquad (1)$$

where λ_0 is the undulator period, γ the beam relativistic factor and $K = 0.94 \times \lambda_0(\mathrm{cm}) \times B_0(\mathrm{T})$ (B_0 is the undulator peak magnetic field) is the so-called deflection parameter. Relation (1) shows the intrinsic tunability, via the tuning of the magnetic field and /or the change of the electron energy, one of the main interests of FELs. During their pathway throughout the undulator and because of the interaction with the electromagnetic field associated to the synchrotron radiation, the electron bunches are submitted to an energy modulation which leads to a spatial micro-bunching at the wavelength λ_{laser} and, as a consequence, to an increase of the coherence of the emitted radiation. The radiation is stored in an optical cavity whose length is chosen so that the round-trip for the photons corresponds to an inter-bunch period. Under given conditions of proper longitudinal and transverse overlap between the photon pulses trapped in the cavity and the electron bunch circulating in the undulator, an energy exchange can occur, via the Lorentz interaction, between the photons and the electrons. The amplification of the optical pulse is possible at the expense of the particles kinetic energy. This leads to an exponential laser amplification which, at some point, is limited by different saturation mechanisms. The saturation is reached when the gain G of the process becomes equal to the losses P of the cavity. The threshold condition ($G > P$), together with the electron beam dynamics, governs the longitudinal behaviour of the laser including the issue (extremely important for FEL applications [2]-[4]) of the macro-temporal and micro-temporal stability.

Table 1: Temporal structure of storage ring FELs

Storage ring	RMS beam size (ps)	RMS laser size (ps)
ACO [15]	300-500	50
Super-ACO [6]	90-300	5-25
UVSOR [7]	57-130	6
VEPP3 [8]	900	90
DUKE [9]	33	3-12
ELETTRA [10]	25	1-5
SOLEIL [11]	10-30	1-5

Storage ring FELs have a complex dynamics because the laser pulse does not interact with a fresh electron bunch (as it happens in LINAC based FEL where the beam is not re-circulated). As a consequence, the improvement of the FEL performances requires a careful study of the nonlinear, strongly coupled laser beam system. The classical approach to the problem [12] does not take into account the different size of the electron bunch and the FEL pulse (see table 1).
Moreover, the FEL induced heating of the longitudinal beam distributions is evaluated in terms of a modification of their RMS value. This means that the distributions are supposed to maintain a gaussian shape (that is the natural solution of the Fokker-Plank equation when the FEL is absent) once the steady state is reached. More recently a numerical model has been proposed [13] which allows a more detailed analysis of the interaction: the beam longitudinal evolution is represented in the Poincaré phase-space and this allows one to put in evidence a shape change of the distributions. Anyway, such a model leads to quantitative results about the maximum laser peak-power which do not have the support of any experimental data.
The model proposed here takes a step further: it is based on a pass to pass analysis of the localised interaction between an electron beam and a shorter laser pulse. This feature allows one to apply it not only to the study of a storage ring FEL but also, for example, to the analysis of the femptosecond X-ray production by means of the interaction of an

electron beam (circulating in a storage ring) with an external laser [14]. In Section 2 the model is presented together with a set of numerical simulations for the FEL installed on the ELETTRA storage ring [10]. In section 3 some experimental and numerical results for the Super-ACO [6] and ACO [15] FELs are compared.

2 FEL-BEAM INTERACTION MODEL AND NUMERICAL SIMULATIONS

Electron beam dynamics in the longitudinal phase-space can be treated by using a two-equations system describing the evolution of the coupled time and energy positions of a single particle with respect to the synchronous one [16]. The effect of the interaction of the electron beam with the storage ring vacuum chamber is taken into account by a term containing an RC impedance model. The laser-beam interaction is considered up to the second order. At the first order of the interaction the micro-bunching of the electron beam takes place and the average energy supplied to the laser wave is zero. At the second order the micro-bunches emit coherent radiation. The laser pulse is assumed to be characterised by a gaussian distribution whose standard deviation is shorter than the electron beam one.

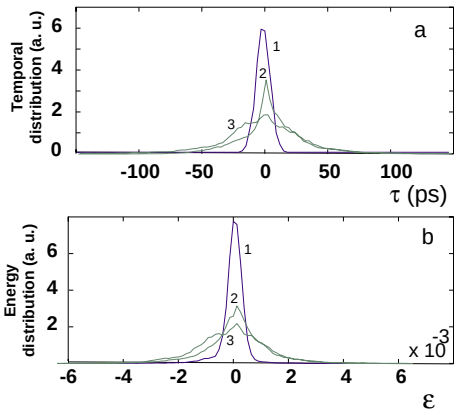

Figure 1: Profiles of the electron temporal (a) and energy (b) distributions for ELETTRA at different times of the dynamic laser evolution: at the beginning of the FEL pulse-rise (curve 1), in the middle of the pulse-rise (curve 2) and in the end of the pulse rise (curve 3).

Figure 1 shows the evolution of the beam temporal and energy distributions for the ELETTRA FEL operated in Q-switched mode. The distributions are gaussian at the beginning of the FEL pulse-rise (curve 1) and becomes more and more distorted as the laser develops (curves 2 and 3). This effect is mainly due to the localised character of the interaction. In fact if the synchotron oscillation period is bigger than the laser pulse rise-time

$$\tau = \frac{T_c}{(G-P)} \qquad (2)$$

(where T_c is the electrons revolution period), that is if the electrons do not have the time to change their position inside the electron distribution during the FEL rise, only those electrons which initially superimpose with the FEL pulse participate to the interaction. This can lead (in the case of ELETTRA) to a flattening or, for more important differences between τ and the synchrotron oscillation period, to a hole burning in both the temporal and energy distributions. The latter is the case of the FEL that will be installed on SOLEIL [11] which has been designed with an electron energy (1.5 GeV) and a laser gain (about 65% for λ_{laser}= 300 nm) bigger than those of ELETTRA (1 GeV and about 40% [10] for λ_{laser}= 300 nm). The synchrotron oscillation is comparable in the two cases (tens of μs). Another important factor which determines the effect of interaction on the beam distributions is, of course, the laser intra-cavity power (few kW both for the ELETTRA and SOLEIL FELs).

3 EXPERIMENTAL RESULTS

Measurements have been performed on the Super-ACO FEL (in Q-switched mode) and on the ACO FEL (operated in cw laser regime) in order to check the presented model. Figure 2a shows a "picture" of the synchrotron radiation (up) emitted by the Super-ACO electrons and of the laser pulse (down) taken by using a double sweep streak camera [17]. A transverse cut of the streak image allows one to represent the longitudinal beam profiles relative to different moments of the interaction (see figure 2b). The initial electron distribution (curve 1) of the Super-ACO bunches is not symmetric because of the wake field. The presence of the FEL stabilises the beam motion [18]: the effect of the wake field disappears (curve 2) and, in accord with numerical simulations (curve 3), the distribution flattens. With respect to the case presented in figure 1, the effect of the localised FEL-beam interaction is less evident. This is mainly due to the important difference between the ELETTRA and Super-ACO laser gains (about 3% for Super-ACO) which leads to different FEL rise-times (fractions of μs for ELETTRA and several μs for SUPER-ACO). The period of the synchrotron oscillation is comparable for the two storage rings (tens of μs).

At the end of the macro-pulse the diffusion process leads the longitudinal distributions back to their original gaussian shape. The electron diffusion time is long if compared to the revolution frequency (hundreds of ns) but smaller than the natural FEL period (few ms) and the synchrotron damping time (tens of ms).

For a FEL operated in its natural (cw) regime, the effect of the localised interaction is in general less spectacular. However a modification of the shape of the electron distribution can be observed (see figure 3). Figure 3a and 3b show the experimental and theoretical behaviours of the longitudinal beam distribution for ACO in absence and in presence of FEL. Simulations are in good agreement with measurements. Figure 3c represents the evolution of the beam energy distribution which is quite close to the temporal one.

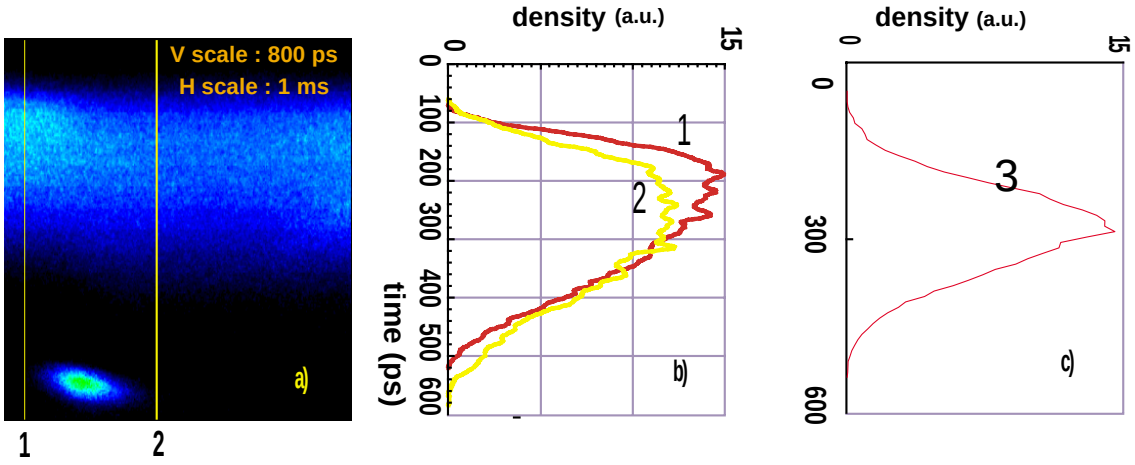

Figure 2: Figure a): Images of the synchrotron radiation (up) emitted by electrons and of the laser pulse (down) by means of a double sweep streak camera. A transverse cut of the image gives the temporal longitudinal distribution at a given time while on the horizontal axis one can follow the evolution of the distribution profile. Figure b): Profiles of the temporal electron distribution at different moments of the interaction. FIgure c): Theoretical profile of the electron temporal distribution at the middle of the FEL rise. For the presented measurements Super-ACO has been operated in Q-switched mode at 800 MeV. The total beam current (divided in two bunches) is 25 mA, allowing a laser gain of about 3%. The FEL wavelength is 300 nm.

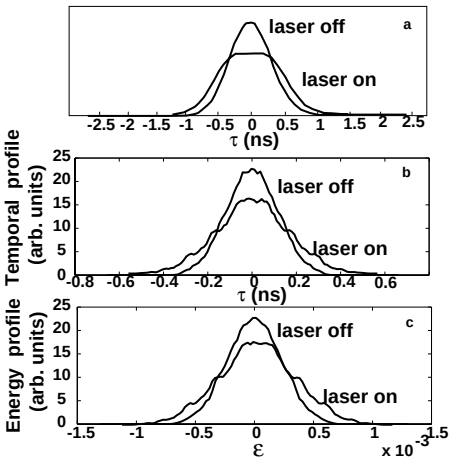

Figure 3: Measurements and simulations for the ACO FEL [5] being operated in cw regime at 220 MeV. The average current is varies from 20 to 150 mA allowing a gain of 0.3 %. The electron bunch distribution has been deduced by using the spectrum analyser acquisition from the signal of a pick-up electrode. Measured temporal distribution (figure a) and simulated temporal (figure b) and energy (figure c) distributions in absence and in presence of the FEL pulse.

4 CONCLUSIONS

The theoretical model presented in this paper is based on a pass to pass analysis of the localised interaction between a short laser pulse with a larger electron distribution. It can be applied, for example, to the study of fs X-ray production and FELs. In this case, one of the main results of the localised interaction is a flattening of both the longitudinal distributions that do not maintain their gaussian profile. Under certain conditions the flattening is accompanied with a hole burning which relaxes through the electron diffusion process. A set of measurements on the Super-ACO and ACO FELs have been performed showing a good agreement with numerical simulations.

REFERENCES

[1] J.M.J. Madey et al., Trans. Nucl. Sci. 20, 980-983 (1973).

[2] M. E. Couprie et al., Rev. of Scient. Inst (1994).

[3] L. Nahon et al., Nucl. Inst. Meth. A. 429, 489-496 (1999).

[4] E. Renault et al., SPIE Proc. 3925, 29-39 (2000).

[5] J. M. Ortéga et al., Nucl. Inst. Meth. A 259, 72-76 (1987).

[6] R. Roux et el., Phys. rev. E 58 n5, 6584-6593 (1998).

[7] H. Hama et al., Nucl. Inst. Meth. A 358, 365-368 (1995).

[8] G. N. Kulipanov et al., Nucl. Inst. Meth. A 296, 1-3 (1990).

[9] V. N. Litvinenko et al., Nucl. Inst. Meth. A 375, 46-52 (1996).

[10] R. Walker et al., Nucl. Inst. Meth. A 429, 179-184 (1999).

[11] M. E. Couprie et al., Nucl. Inst. Meth. B 144, 66-74 (1998).

[12] G. Dattoli, A. Renieri, Nuovo Cimento B59, 39 (1980).

[13] V. N. Litvinenko et al., Nucl. Inst. Meth. A 375, 46-52 (1999).

[14] A. A. Zholents, M. S. Zolotorev, Phys. Rev. Lett. 76 6, 1652 (1983).

[15] M. Billardon et al., Phys. Rev. Lett. 51, 1652 (1983).

[16] M. Sands, SLAC Rep.121 (1970).

[17] R. Roux et al., Nucl. Inst. Meth. A 393, 179 (1997).

[18] G. Dattoli et al., Phys. Rev. E 58 5, 6570-6574 (1998).